Preferential Accumulation of ^{3}H-Tetraphenylphosphonium in Non–Small Cell Lung Carcinoma in Mice: Comparison with ^{99m}Tc-MIBI

Igal Madar, PhD[1]; Lola Weiss, PhD[2]; and Gabriel Izbicki, MD[3]

[1]Department of Medical Biophysics and Nuclear Medicine, Hadassah University Medical Center, Jerusalem, Israel; [2]Department of Immunology, Hadassah University Medical Center, Jerusalem, Israel; and [3]Department of Pulmonary Research, Hadassah University Medical Center, Jerusalem, Israel

We have previously shown enhanced accumulation of the delocalized lipophilic cation ^{11}C-triphenylmethylphosphonium in canine brain glioma, suggesting its potential use for tumor staging in humans using PET. Here, we extend our studies of phosphonium cations to nonbrain tumors and characterize the biodistribution and tumor specificity of ^{3}H-tetraphenylphosphonium (^{3}H-TPP) in non–small cell lung carcinoma in mice. **Methods:** ^{3}H-TPP accumulation in isolated malignant lung nodules of the Lewis lung carcinoma (LLC) cell line, in LLC-bearing lung, and in control lung was measured at various intervals after inoculation. Tumor uptake and biodistribution of ^{3}H-TPP were compared with those of ^{99m}Tc-methoxyisobutylisonitrile (MIBI). **Results:** ^{3}H-TPP accumulation in LLC nodules at 14 d was significantly greater than that in controls, peaked at 21 d, and declined to lower values at 28 d after injection. At 21 d after injection, ^{3}H-TPP uptake in LLC nodules was greater than that in control lung tissue and in LLC-bearing lung tissue—by 549% and 230%, respectively—whereas ^{99m}Tc-MIBI nodule uptake was greater by 90% and 30%, respectively. **Conclusion:** The high tumor accumulation and sensitivity to the phase of tumor development suggest the potential use of radiolabeled phosphonium analogs for in vivo tumor staging and as a tool for investigating tumor evolution.

Key Words: tetraphenylphosphonium; non–small cell lung carcinoma; mouse model

J Nucl Med 2002; 43:234–238

In recent years, the mitochondria as the site of genetic mutations associated with carcinogenesis and the place where early steps of apoptosis occur has attracted much attention (*1–3*). Genetic mutations and apoptosis are associated with changes in the mitochondrial membrane potential ($\Delta\Psi_m$) (*3*). Delocalized lipophilic cations such as ^{3}H-tetraphenylphosphonium (^{3}H-TPP) are a standard tool for measurements of $\Delta\Psi_m$ in vitro (*4*). The lipophilicity of the cation allows ^{3}H-TPP to move freely through the membrane lipid bilayer by passive diffusion into the mitochondrial matrix. The delocalized positive charge allows the cation to equilibrate with the transmembrane electric gradient, as a function of the Nernst equation.

Uptake studies on culture preparations of the human breast carcinoma MCF-7 cell line have shown that ^{3}H-TPP accumulates in malignant cells >30 times more than in normal epithelial cells (*5*). Depolarization of the membrane potential by a high level of potassium revealed that the cation accumulates mainly in the mitochondria. Subsequent studies corroborated the preferential uptake of ^{3}H-TPP in a wide spectrum of malignant cell lines (*6–12*). Microelectrode recordings have shown that the preferential accumulation of ^{3}H-TPP is associated with increased membrane potential of malignant cells (*6,13*). Thus, the development of radiolabeled phosphonium cations as a noninvasive imaging tool may also serve as an effective molecular probe for investigating the role of mitochondria in the pathophysiology and treatment of cancer and as a staging tool in diagnostic imaging of solid tumors.

Previously, we evaluated the kinetics and tumor selectivity of the positron-emitting phosphonium cation ^{11}C-triphenylmethylphosphonium (^{11}C-TPMP) in canine brain glioma using PET (*14*). ^{11}C-TPMP exhibits a high tumor-to-nontumor ratio. ^{11}C-TPMP accumulation is 44.5 times greater in tumor tissue than in the contralateral normal brain. This tumor contrast is 1 order of magnitude greater than that reported for glioma studies on humans for other available PET and SPECT cations, including ^{99m}Tc-methoxyisobutylisonitrile (MIBI) (*15*), ^{82}Rb (*16*), and ^{201}Tl (*17*). ^{11}C-TPMP exhibits several features characterizing a good probe for tumor imaging, including rapid clearance from the blood pool, rapid tumor uptake, fast equilibrium of tracer in tumors, and prolonged retention in tumors. Patlak analysis

Received Apr. 2, 2001; revision accepted Oct. 15, 2001.
For correspondence or reprints contact: Igal Madar, PhD, Division of Nuclear Medicine, Department of Radiology, Johns Hopkins University School of Medicine, 601 N. Caroline St./JHOC 4230, Baltimore, MD 21282-0885.
E-mail: imadar@receptor.rad.jhu.edu

suggests that over a 20- to 95-min interval, the tracer remains in the tumor with minimal washout (*14*).

^{11}C-TPMP, similar to other cationic radiopharmaceuticals, has a poor blood–brain barrier permeability. Thus, the uptake ratio of tumor to contralateral brain is not a true measure of tracer tumor selectivity. Here, we extend our studies of radiolabeled phosphonium cations and characterize the biodistribution and tumor selectivity of ^{3}H-TPP in the mouse model of Lewis lung carcinoma (LLC), a non–small cell lung carcinoma line. The multitude of information gained with ^{3}H-TPP in vitro is useful for identification of cell lines suitable for in vivo studies. The LLC model allows direct measurement of the ratio of tumor activity to background activity. We compared the biodistribution and tumor selectivity of ^{3}H-TPP with ^{99m}Tc-MIBI. The delocalized lipophilic cation ^{99m}Tc-MIBI is a widely used imaging probe in the clinical setting (*18*). Similar to ^{3}H-TPP, ^{99m}Tc-MIBI accumulates in the mitochondria in a $\Delta\Psi_m$-dependent manner. Thus, comparison of ^{3}H-TPP with ^{99m}Tc-MIBI permits assessment of the potential clinical utility of phosphonium cations.

MATERIALS AND METHODS

Preparation of LLC Cell Culture

Studies of the radiolabeled phosphonium cation ^{3}H-TPP (NEN Life Science, Boston, MA) and ^{99m}Tc-MIBI were performed on LLC cells (American Type Culture Collection, Manassas, VA). Cells were grown in 75-cm^2 tissue-culture flasks at 37°C in 5% CO_2 and 95% air in 97% humidity. The culture medium was Dulbecco's modified Eagle's medium supplemented with 2 mmol/L L-glutamine, penicillin/streptomycin (50 IU/L, Gibco, Grand Island, NY), and 10% heat-inactivated newborn calf serum (Sigma, St. Louis, MO). Cells adherent to the culture dish were harvested with 0.05% trypsin and 0.53 mmol/L ethylenediaminetetraacetic acid (Gibco) and were washed with cold culture medium. After being incubated for 2 h in ice-cold medium, the cells were washed once in unsupplemented medium to remove the serum. The cells were counted using a hemocytometer and suspended at a concentration of 10^6/mL for uptake studies. Cell viability was determined with trypan blue.

Preparation of ^{99m}Tc-MIBI

^{99m}Tc-MIBI was prepared by adding $^{99m}TcO_4^-$ (1 mL, 740–1,110 MBq) obtained from a commercial ^{99}Mo/^{99m}Tc generator (Cardiolite; DuPont Merck Pharmaceuticals, Billerica, MA) and heating the mixture at 100°C for 10 min. The preparation was purified to remove excess free ligand with a Sep-Pak cartridge (Waters, Milford, MA) as previously described (*19*). Radiochemical purity was ≥96%.

In Vivo Uptake Studies

Uptake studies were performed in parallel on age-matched tumor-bearing and control male C57Bl mice (body weight, 21.5 ± 3.7 g). LLC cells (5×10^5 in a volume of 0.5 mL phosphate-buffered saline) were injected through a tail vein. In the lung parenchyma, LLC cells create vascularized nodules (approximately 2 mm in diameter) that can be dissected individually. At various intervals after tumor inoculation, uptake studies were performed (3–5 mice per interval, 2 repetitions). ^{3}H-TPP (74 kBq) and ^{99m}Tc-MIBI (3,700 kBq) were injected, either separately or together, through the tail vein in 0.2 mL saline. The animals were decapitated, and the lungs and major organs were removed together and placed on ice. Blood samples were collected by cardiac puncture. The lungs were placed on a cold plate under a binocular, the major blood vessels were removed, and individual nodules were dissected (10–20 nodules per lung). ^{3}H-TPP and ^{99m}Tc-MIBI radioactivity was measured in LLC nodules, the remaining lung tissue of the LLC-bearing lungs, and lungs dissected from non–tumor-bearing mice (control lungs). ^{3}H-TPP and ^{99m}Tc-MIBI activity was counted separately in similar volumes of tissue sample. For counting ^{99m}Tc-MIBI radioactivity, tissue was placed immediately in vials in a scintillation γ-counter. The energy window was 100–190 keV. Standards (1/100 of the injectate) were placed at the beginning of each study. For counting ^{3}H-TPP radioactivity, tissue was dissolved overnight in 1 mL protosol (NEN Life Science) and counted along with standards (1/1,000).

Data Analysis

Results were expressed as percentage injected dose per gram of tissue (%ID/g). The significance of a change in cation uptake over postinoculation time was determined by factorial ANOVA using 2 repeated variables: time (3, 7, 10, 17, 20, and 24 d) and tissue (malignant vs. control). At each postinjection interval, 2 repeated studies were performed and their results were pooled for statistical analysis. The significance of differences between ^{3}H-TPP and ^{99m}Tc-MIBI was analyzed first by calculating the ratio of uptake in tumor to uptake in normal lung and then by performing repeated-measures ANOVA using 2 variables: time (14, 21, and 28 d) and tracer (^{3}H-TPP and ^{99m}Tc-MIBI). Posthoc Tukey tests were used to localize the time points of significant change as determined by ANOVA. The level of significance was determined by a 2-tailed *t* test, performed at the points of significant change as indicated by Tukey testing, and was $P < 0.05$.

RESULTS

Biodistribution Studies

Figure 1 depicts the time–activity curves of ^{3}H-TPP and ^{99m}Tc-MIBI in the lungs of control mice. At 5 to 120 min after injection, ^{3}H-TPP and ^{99m}Tc-MIBI exhibited a similar washout rate, with plateau concentrations obtained at approximately 60 min after injection. ^{3}H-TPP lung uptake was significantly higher than ^{99m}Tc-MIBI at all time points. The biodistribution studies in mice showed significant differences between ^{3}H-TPP and ^{99m}Tc-MIBI (Table 1). The initial activity of ^{3}H-TPP in most major organs was greater than that of ^{99m}Tc-MIBI. At 5 min, ^{3}H-TPP activity in the heart, liver, lung, and spleen was significantly greater than ^{99m}Tc-MIBI activity, but in the kidney ^{3}H-TPP activity was much smaller than ^{99m}Tc-MIBI activity, suggesting faster renal clearance of ^{3}H-TPP than of ^{99m}Tc-MIBI. At 120 min, ^{3}H-TPP activity in the liver was similar to ^{99m}Tc-MIBI activity, indicating a similar hepatobiliary clearance rate for both cations.

^{3}H-TPP and ^{99m}Tc-MIBI Uptake in LLC Tumor

Table 2 summarizes the accumulation of ^{3}H-TPP in control lung, LLC-bearing lung (LLC lung), and isolated nodules (LLC nodules) at several time points after tumor inoc-

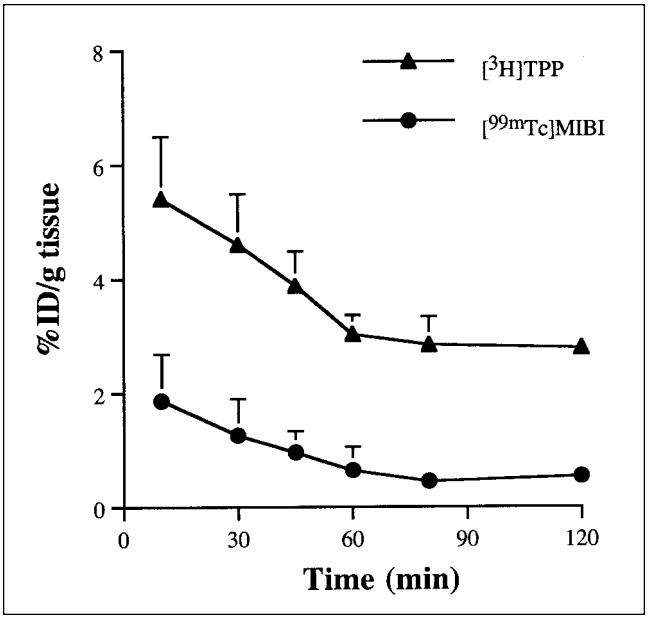

FIGURE 1. Time–activity curves of ^{3}H-TPP and ^{99m}Tc-MIBI in mouse lung.

ulation. Significant differences between LLC lung and control lung ($P \leq 0.034$), LLC nodules and control lung ($P \leq 0.0027$), and LLC nodules and LLC lung ($P \leq 0.011$) were observed at 17, 20, and 24 d after inoculation. ^{3}H-TPP accumulation in LLC nodules reached a peak at 20 d after inoculation and declined to significantly ($P = 0.0038$) lower values thereafter. At 20 d, ^{3}H-TPP activity was 4.1 times greater in LLC nodules than in control lung and 2.1 times greater in LLC nodules than in LLC lung.

Table 3 summarizes the accumulation of ^{3}H-TPP and ^{99m}Tc-MIBI in control lung, tumor-bearing lung, and isolated nodules 14, 21, and 28 d after inoculation. Both tracers exhibited increased uptake in the malignant tissue. Significant differences between ^{3}H-TPP and ^{99m}Tc-MIBI accumulation in isolated LLC nodules were found at all studied postinoculation time points ($P < 0.037$). Similarly, the uptake ratio of LLC nodules to LLC lung was significantly ($P < 0.041$) greater for ^{3}H-TPP than for ^{99m}Tc-MIBI at 14 (2.5:1) and 21 d (5.5:1) but not at 28 d ($P = 0.26$). In the tumor-bearing lung, the ^{3}H-TPP/^{99m}Tc-MIBI ratio was highest at 14 d (2.8:1) and had gradually declined at 21 d (2.5:1) and 28 d (1.8:1). No significant differences ($P > 0.073$) in the uptake ratio of LLC lung to control lung were found between ^{3}H-TPP and ^{99m}Tc-MIBI. ^{3}H-TPP accumulation in the normal lung parenchyma was approximately twice that of ^{99m}Tc-MIBI at all postinoculation time points studied ($P < 0.05$).

TABLE 1
Biodistribution of Lipophilic Cations in Mice

Site	5 min after administration		120 min after administration	
	^{3}H-TPP	^{99m}Tc-MIBI	^{3}H-TPP	^{99m}Tc-MIBI
Blood	0.13 ± 0.02	0.41 ± 0.04	0.09 ± 0.02	0.26 ± 0.05
Brain	0.09 ± 0.04	0.08 ± 0.03	0.06 ± 0.02	0.08 ± 0.04
Heart	24.50 ± 4.72	9.07 ± 1.26	20.70 ± 1.92	5.08 ± 0.25
Lung	5.41 ± 0.35	2.11 ± 0.51	2.81 ± 0.41	0.98 ± 0.19
Liver	9.09 ± 0.53	6.85 ± 1.18	6.12 ± 1.08	5.55 ± 1.08
Spleen	3.30 ± 0.25	1.84 ± 0.41	1.93 ± 0.47	1.27 ± 0.33
Kidney	6.11 ± 0.44	27.90 ± 3.77	4.37 ± 0.66	12.60 ± 2.57
Muscle	3.05 ± 0.72	2.44 ± 0.23	2.22 ± 0.41	1.56 ± 0.31

Data are mean (±SD) %ID/g.

TABLE 2
^{3}H-TPP Accumulation in Lewis Lung Carcinoma in Mice 60 Minutes After Intravenous Administration of 74 kBq Tracer

Time after inoculation (d)	Control lung	LLC lung	LLC nodules	(T − C)/C (%)
3	2.43 ± 0.32	2.25 ± 0.23		
7	2.09 ± 0.36	2.46 ± 0.32		
10	2.73 ± 0.38	2.56 ± 0.38		
17	2.08 ± 0.40	3.27 ± 0.39	5.62 ± 0.79	170
20	1.81 ± 0.39	3.84 ± 0.52	9.26 ± 1.20	412
24	1.76 ± 0.30	2.60 ± 0.34	3.99 ± 0.65	127

(T − C)/C = (LLC nodule − control lung)/control lung.
Data are mean (±SD) %ID/g.

DISCUSSION

The major finding of this set of studies was the high tumor selectivity of ^{3}H-TPP in the mouse model of small cell lung carcinoma. Radioactivity in ^{3}H-TPP nodules was greater than radioactivity in control lung by nearly 500%, and ^{99m}Tc-MIBI nodule activity was greater by 90%. Furthermore, the longitudinal set of studies of tumor uptake across postinoculation time points revealed that ^{3}H-TPP accumulation was sensitive to tumor progression, as reflected by the parabolic relationship between tumor age and ^{3}H-TPP uptake. ^{99m}Tc-MIBI showed a similar biphasic pattern, although to a lesser extent.

The biodistribution studies showed the fast clearance of ^{3}H-TPP from the blood pool, an essential feature of an imaging tracer. At 5 min, ^{3}H-TPP blood radioactivity was very low—close to radioactivity measured in the brain tissue, an organ impermeable to lipophilic cations—suggesting that most of the TPP radioactivity had already cleared from the blood pool. This finding is in line with results obtained from a PET study on dogs, in which ^{11}C-TPMP plasma radioactivity declined to nearly zero within 2 min after injection (*14*). ^{3}H-TPP accumulation was most intense in the myocardium, which has a high density of mitochondria, and was lowest in the spleen, which has a low

TABLE 3
^{3}H-TPP and ^{99m}Tc-MIBI Uptake in Lewis Lung Carcinoma in Mice 60 Minutes After Intravenous Administration of 74 kBq Tracer

Time after inoculation (d)	Control lung	LLC lung	LLC nodule	(T − C)/C (%)	TPP/MIBI
^{3}H-TPP					
14	2.12 ± 0.32	3.41 ± 0.39	4.91 ± 0.64	132	2.55
21	1.74 ± 0.39	3.19 ± 0.52	10.40 ± 1.02	498	5.47
28	1.66 ± 0.31	2.12 ± 0.34	2.95 ± 0.46	78	1.04
^{99m}Tc-MIBI					
14	0.91 ± 0.21	1.20 ± 0.33	1.38 ± 0.51	52	
21	0.86 ± 0.18	1.28 ± 0.48	1.64 ± 0.32	91	
28	0.75 ± 0.14	1.14 ± 0.51	1.31 ± 0.44	75	

(T − C)/C = (LLC nodule − control lung)/control lung.
Data are mean (±SD) %ID/g.

density of mitochondria. In the heart, ^{3}H-TPP accumulation was much more pronounced than ^{99m}Tc-MIBI accumulation as measured in this and other studies (*19*). ^{3}H-TPP uptake was significantly ($P < 0.05$) greater than ^{99m}Tc-MIBI uptake in the lung and liver. This finding suggests a more potent accumulation of ^{3}H-TPP than of ^{99m}Tc-MIBI in mitochondria.

^{3}H-TPP exhibited a stronger accumulation in malignant tissue and a greater tumor-to-nontumor ratio than did ^{99m}Tc-MIBI. The higher accumulation of ^{3}H-TPP contrasted with its lower lipophilic nature (log $P = 1.2$ (*20*)), compared with MIBI (log $P = 2.89$ (*19*)). Increased lipophilicity within a certain range facilitates the inward transport of positively charged ions through the membrane lipid bilayer, as has been shown for several lipophilic cations, including technetium complexes and phosphonium cations (*19–21*). Alternatively, the better extraction of ^{3}H-TPP in tumors may be dictated by factors other than lipophilicity, such as molecular size and density of formal charge (*22*).

Several groups have studied the pharmacokinetics of lipophilic cationic technetium complexes in normal and malignant cells (*19,23–25*). ^{99m}Tc-MIBI accumulation 2 h after administration was 0.5 %ID/g in kidney, liver, and subcutaneous xenografts in mice (*19*). This uptake level was below that observed in lung carcinoma in this study (1.28 %ID/g). The reduced accumulation of ^{99m}Tc-MIBI in the kidney and liver tumor models may result from lesser vascularization in these models, as compared with the lung model, whose nodules are surrounded by the rich parenchymal capillary bed. Uptake studies of several cationic technetium isonitrile complexes in subcutaneous tumor models have shown low tumor-to-muscle ratios (<1:1) for all studied cations, including ^{99m}Tc-MIBI (*19,23*). ^{3}H-TPP accumulation was 4.1 times greater in LLC tumor than in muscle tissue. Muscle activity was taken as a reference for comparison of tracers because of the lack of a host tissue in subcutaneous models. In subcutaneous breast tumors in rats, uptake of ^{99m}Tc-MIBI was 2 and 5 times that of the cations ^{99m}Tc-tetrofosmin and ^{99m}Tc-Q12, respectively (*24*). The current study suggests that tumor selectivity is greater for ^{3}H-TPP than for ^{99m}Tc-MIBI and other lipophilic cationic technetium complexes.

An additional interesting finding derived from the longitudinal uptake study across tumor postinoculation times was the biphasic change in ^{3}H-TPP accumulation in LLC nodules. ^{3}H-TPP accumulation increased from day 14 to day 21 after inoculation and decreased at 28 d after inoculation. The reasons for the parabolic change in ^{3}H-TPP tumor uptake are not clear. At 28 d after injection, the lung is densely infested with malignant nodules and the decreased uptake may be caused by the lagging of vascularization behind the rapid growth of the malignant cells, thereby affecting tracer delivery and resulting in necrotic or apoptotic processes. Both reduced delivery and cell death would lead to a decrease in uptake of the lipophilic cation. However, no necrotic core was observed in individual nodules. Alternatively, the change in ^{3}H-TPP tumor uptake may reflect alterations in tumor aggressiveness. An approach to the saturation level in the distribution of LLC cells in the lung may slow the cell proliferation rate. Several lines of evidence suggest that ^{3}H-TPP uptake in malignant cells may correlate with tumor cell proliferation rate. In dispersed cells of biopsy samples, ^{3}H-TPP uptake was 3 times greater in grade III glioma than in meningiomas (*7*). Depolarization of membrane potential resulted in a marked inhibition of cell proliferation associated with depletion of ^{3}H-TPP cellular content in T cell and MCF-7 cell lines (*26–29*). Thus, the parabolic change in ^{3}H-TPP uptake may reflect parallel changes in the rate of tumor cell proliferation: an increase at earlier stages of tumor development and a decrease at later stages, when the lung is saturated with malignant cells. At advanced stages of tumor development, apoptotic or necrotic processes involving collapse of the mitochondrial membrane potential and a subsequent decrease in mitochondrial ^{3}H-TPP accumulation (*3*) may take place.

CONCLUSION

^{3}H-TPP showed high tumor selectivity in an in vivo non–small cell lung carcinoma model. This finding supports our previous observations of the promising diagnostic utility of positron-emitting phosphonium analogs as imaging tracers for tumor staging in humans. The sensitivity of ^{3}H-TPP to tumor age suggests that phosphonium cations may be useful as in vivo probes for characterizing molecular changes during tumor evolution.

REFERENCES

1. Cavalli LR, Liang BC. Mutagenesis, tumorigenicity, and apoptosis: are the mitochondria involved? *Mutat Res*. 1998;398:19–26.
2. Wallace DC. Mitochondrial diseases in man and mouse. *Science*. 1999;283: 1482–1488.
3. Kroemer G, Dallaporta B, Resche-Rigon M. The mitochondrial death/life regulator in apoptosis and necrosis. *Ann Rev Physiol*. 1998;60:619–642.
4. Hockings PD, Rogers PJ. The measurement of transmembrane electrical potential with lipophilic cations. *Biochim Biophys Acta*. 1996;1282:101–106.
5. Davis S, Weiss MJ, Wong JR, Lampidis TJ, Chen LB. Mitochondrial and plasma membrane potentials cause unusual accumulation and retention of rhodamine 123 by human breast adenocarcinoma-derived MCF-7 cells. *J Biol Chem*. 1985;260: 13844–13850.
6. Lampidis TJ, Hasin Y, Weiss MJ, Chen LB. Selective killing of carcinoma cells "in vitro" by lipophilic-cationic compounds: a cellular basis. *Biomed Pharmacother*. 1985;39:220–226.
7. Steichen JD, Weiss MJ, Elmaleh DR, Martuza RL. Enhanced in vitro uptake and retention of ^{3}H-tetraphenylphosphonium by nervous system tumor cells. *J Neurosurg*. 1991;74:116–122.
8. Arcangeli A, Olivotto M. Plasma membrane potential of murine erythroleukemia cells: approach to measurement and evidence for cell-density dependence. *J Cell Physiol*. 1986;127:17–27.
9. Sanchez Olavarria J, Galindo C, Montero M, Baquero Y, Victorica J, Satrustegui J. Measurement of 'in situ' mitochondrial membrane potential in Ehrlich ascites tumor cells during aerobic glycolysis. *Biochim Biophys Acta*. 1988;935:322–332.
10. Andrews PA, Albright KD. Mitochondrial defects in cis-diamminedichloroplatinum(II)-resistant human ovarian carcinoma cells. *Cancer Res*. 1992;52:1895–1901.
11. Rideout D, Bustamante A, Patel J. Mechanism of inhibition of FaDu hypopharyngeal carcinoma cell growth by tetraphenylphosphonium chloride. *Int J Cancer*. 1994;57:247–253.
12. Dong Y, Berners-Price SJ, Thorburn DR, et al. Serine protease inhibition and mitochondrial dysfunction associated with cisplatin resistance in human tumor cell lines: targets for therapy. *Biochem Pharmacol*. 1997;53:1673–1682.
13. Lichtshtein D, Kaback HR, Blume AJ. Use of a lipophilic cation for determination of membrane potential in neuroblastoma-glioma hybrid cell suspensions. *Proc Natl Acad Sci USA*. 1979;76:650–654.
14. Madar I, Anderson JH, Szabo Z, et al. Enhanced uptake of [^{11}C]TPMP in canine brain tumor: a PET study. *J Nucl Med*. 1999;40:1180–1185.
15. Park CH, Kim SM, Zhang JJ, Intenzo CM, McEwan JR. Tc-99m MIBI brain SPECT in the diagnosis of recurrent glioma. *Clin Nucl Med*. 1994;19:57–58.
16. Doyle WK, Budinger TF, Valk PE, Levin VA, Gutin PH. Differentiation of cerebral radiation necrosis from tumor recurrence by [^{18}F]FDG and ^{82}Rb positron emission tomography. *J Comput Assist Tomogr*. 1987;11:563–570.
17. Kim KT, Black KL, Marciano D, et al. Thallium-201 SPECT imaging of brain tumors: methods and results. *J Nucl Med*. 1990;31:965–969.
18. Salvatore M, Del Vecchio S. Dynamic imaging: scintimammography. *Eur J Radiol*. 1998;27(suppl):S259–S264.
19. Barbarics E, Kronauge JF, Davison A, Jones AG. Uptake of cationic technetium complexes in cultured human carcinoma cells and human xenografts. *Nucl Med Biol*. 1998;25:667–673.
20. Lampidis TJ, Shi YF, Calderon CL, Kolonias D, Tapiero H, Savaraj N. Accumulation of simple organic cations correlates with differential cytotoxicity in multidrug-resistant and -sensitive human and rodent cells. *Leukemia*. 1997;11: 1156–1159.
21. McKeage MJ, Berners-Price SJ, Galettis P, et al. Role of lipophilicity in determining cellular uptake and antitumour activity of gold phosphine complexes. *Cancer Chemother Pharmacol*. 2000;46:343–350.
22. Burns RJ, Murphy MP. Labeling of mitochondrial proteins in living cells by the thiol probe thiobutyltriphenylphosphonium bromide. *Arch Biochem Biophys*. 1997;339:33–39.
23. Packard AB, Barbarics E, Kronauge JF, Wen PY, Day PJ, Jones AG. Comparison of uptake of ^{99m}Tc-alkylisonitriles in the rat 9L gliosarcoma tumor model. *Nucl Med Biol*. 1997;24:21–25.
24. Bernard BF, Krenning EP, Breeman WA, et al. ^{99m}Tc-MIBI, ^{99m}Tc-tetrofosmin and ^{99m}Tc-Q12 in vitro and in vivo. *Nucl Med Biol*. 1998;25:233–240.
25. Friebe M, Mahmood A, Spies H, et al. '3+1' mixed-ligand oxotechnetium(V) complexes with affinity for melanoma: synthesis and evaluation in vitro and in vivo. *J Med Chem*. 2000;43:2745–2752.
26. Gelfand EW, Cheung RK, Grinstein S. Role of membrane potential in the regulation of lectin-induced calcium uptake. *J Cell Physiol*. 1984;121:533–539.
27. Gelfand EW, Cheung RK, Mills GB, Grinstein S. Role of membrane potential in the response of human T lymphocytes to phytohemagglutinin. *J Immunol*. 1987; 138:527–531.
28. Strobl JS, Wonderlin WF, Flynn DC. Mitogenic signal transduction in human breast cancer cells. *Gen Pharmacol* 1995;26:1643–1649.
29. Wang S, Melkoumian Z, Woodfork KA, et al. Evidence for an early G1 ionic event necessary for cell cycle progression and survival in the MCF-7 human breast carcinoma cell line. *J Cell Physiol*. 1998;176:456–464.